ARTICLE NO. 79-2004R

Foilborne Hydrodynamic Performance of Jetfoil®

A. E. Noreen,* P. R. Gill,† and W. M. Feifel‡
Boeing Marine Systems, Seattle, Wash.

The Boeing Jetfoil Model 929-115 hydrofoil ship was derived from Model 929-100, with increased forward foil area for larger load-carrying capacity. Forward and aft foil contours were revised to increase cavitation margin. New hydrodynamic design methods were employed to maximize foil thickness for minimum structural weight. Prediction of foilborne cruise performance was based upon theoretical analysis, model test data, and full-scale trial data from Model 929-100. Extensive flowfield observations were made of the foil systems during sea trials of the first Model 929-115 produced. Good agreement was found between predicted and observed cavitation and ship performance characteristics. Sensitivity of ship performance to operating variables was determined from sea trial data.

Nomenclature

C = chord length
C_ℓ = section lift coefficient
C_L = foil lift coefficient
C_P = pressure coefficient
H = forward foil depth, ft
t = maximum section thickness
V = ship speed, knots
Y = transverse coordinate
Z = axial coordinate
α = angle of attack
δ = flap deflection
θ = pitch angle
σ = standard deviation

Introduction

THE Jetfoil§ hydrofoil ship is designed to cruise in 12 ft waves at 45 knots while giving its occupants a smooth ride. The ship features water jet propulsion, fully submerged foils in canard arrangement, and an automatic stabilization and control system actuating trailing-edge flaps. Jetfoil Model 929-115 was derived from Jetfoil Model 929-100,[1] which has been in commercial service since 1975. This operational experience provided a well-founded base for design and performance prediction of the new, improved craft. Forward foil area was increased to provide larger load-carrying capacity. Contour of all foils was revised to increase cavitation margin. The model 929-115 foil system structure was designed for increased fatigue and flaw growth life. Advanced hydrodynamic design methods were employed to maximize foil thickness with minimum structural weight. Prediction of foilborne cruise performance of the Model 929-115 was based upon theoretical analysis, model test data, and full-scale Model 929-100 sea trial results.

Sea trials were conducted on Jetfoil 0011, the first Model 929-115 produced, in July through October 1978. Ship performance was determined, and the flow over the foil system was observed to detect cavitation or ventilation. Good agreement was found between theoretical predictions and sea trial results. Sensitivity of the ship speed-power relationship to operating variables such as ship weight, sea condition, foil depth, and foil angle of attack was determined from sea trial data.

Presented as Paper 79-2004 at the AIAA/SNAME Advanced Marine Vehicles Conference, Baltimore, Md., Oct. 2-4, 1979; submitted Nov. 6, 1979; revision received March 13, 1980.

Index categories: Marine Vessel Systems, Submerged and Surface; Marine Hydrodynamics; Vessel and Control Surface.

*Manager, Hydrodynamics. Member AIAA.
†Naval Architect.
‡Hydrodynamic and Aerodynamic Engineer. Member AIAA.

§Jetfoil is a registered trademark of the Boeing Company.

Hydrodynamic Design Objectives

Several objectives guided the hydrodynamic redesign of the foil system for Model 929-115. These were, in order of importance:

1) Compatibility with increased structural fatigue life requirements.

2) Increased full-load dynamic lift by 3 long tons.

3) A forward foil cavitation-free at 45 knots ship speed and full-load dynamic lift.

4) Improved aft foil cavitation margins.

Configuration Description

The principal hydrodynamic configuration changes between Models 929-100 and 929-115 are shown in Fig. 1.

The Model 929-100 forward foil, shown in Fig. 2, had a rectangular planform and used a conventional foil section of 7.5% thickness. The intersection between the forward strut and foil was formed by a straight-sided pod. The forward foil system designed for Jetfoil Model 929-115, shown in Fig. 2, used a tapered planform and contoured pod. Forward foil area was increased over that of Model 929-100, as shown in Fig. 3, to permit a ship weight increase. Foil planform and the foil section shapes, varying in thickness from 8.75% at the root to 6.5% at the tip, were chosen to minimize structural weight. The more complex shape was feasible for Model 929-115 because of the selection of numerical machining to contour the forward foil.

The Model 929-115 Jetfoil pod was carefully contoured to minimize perturbation of chordwise pressure distribution caused by mutual interference between foil system components. For this purpose, the pod was lengthened and locally enlarged in the nose and tail section to achieve an appropriate shape. The Model 929-115 pod was placed so that the lower surface of the foil, which carries the highest tension loads, was left exposed for easy inspection.

The forward strut chord was lengthened from 45 to 50 in., the basic section thickness was increased from 12 to 13.5%, and the spanwise thickness distribution was changed. The section shape was modified to improve cavitation characteristics.

Changes to the aft foil system were less extensive than to the forward foil system. Foil planform, strut shape, and pod

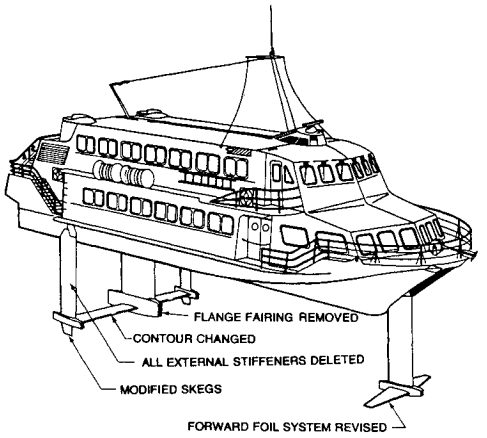

Fig. 1 Model 115 Jetfoil (principal hydrodynamic change from Model 929-100).

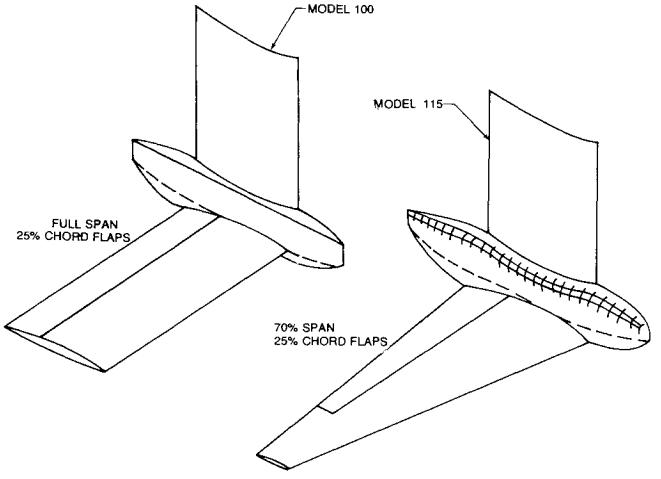

Fig. 2 Forward foil system (starboard half only shown).

shapes remained virtually unchanged. All external structural stiffeners were removed. Aft foil thickness for Model 929-115 was increased near the center pod, where the bending loads are largest. The basic foil shape was slightly modified from that of Model 929-100 by increasing the camber and changing the foil thickness distribution.

Hydrodynamic Foil Design Technique

Techniques proven in the design of advanced transonic airfoils and of high-performance laminar-flow airfoil sections for gliders were adapted for development of the Model 929-115 forward foil section. The sections were contoured to provide the lowest possible pressure, limited by the onset of cavitation, over a large portion of the foil upper surface. For additional foil lift, a region of high pressure was provided on the aft lower surface of the foil sections. This type of chordwise pressure distribution yielded, for a given minimum pressure level, foil section shapes that exhibited a fair amount of aft camber and were thicker than the conventional sections of Model 929-100, as shown in Fig. 3.

Three-dimensional potential flow computer programs[2,3] were used to obtain spanwise load distributions for initial design of the section camber lines and to design a contoured pod to minimize section interference. The programs used a panel method that determines the shape of and/or the forces acting on bodies. The method of images accounted for the presence of a free water surface.

The foil sections were designed with the aid of a two-dimensional mixed boundary conditions potential flow

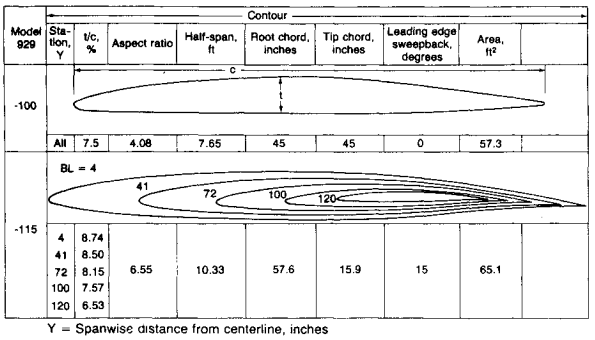

Fig. 3 Forward foil comparison.

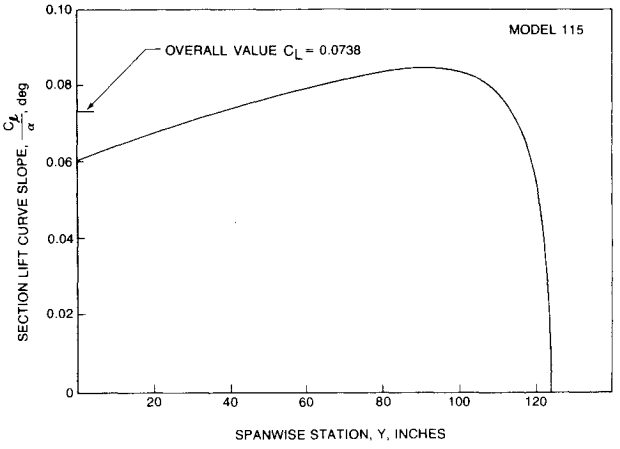

Fig. 4 Spanwise variation of front foil local lift coefficient.

computer program.[4] In this program, part of the section geometry can be held fixed while the velocity distribution is prescribed for the rest of the section. The program determines the shape required to yield this prescribed velocity distribution and, at the same time, determines the velocity distribution about the fixed portion of the foil section. For fine tuning of section contours and for cavitation regime analysis at off-design conditions, a two-dimensional potential flow analysis computer program[5] was employed. It uses an influence coefficient method where the bodies are approximated by a polygon of panels carrying a linearly varying vortex and/or source distribution. Velocities, pressures, and forces acting on the configuration surfaces are calculated. Part of the program is a geometry manipulation package, which can generate the geometry for foils with a deflected trailing-edge flap.

Avoidance of cavitation was a prime concern in the shaping of hydrodynamic contours. At a design speed of 45 knots and 6 ft foil depth in 59°F seawater, the calculated pressure coefficient for the onset of vaporous cavitation was −0.43. This value was used as the minimum allowable pressure coefficient for the design of new shapes.

Forward Foil Design

Forward foil area and span were enlarged for higher load-carrying capability and lower induced drag. Planform and taper ratio were selected for minimum foil system weight. Once the planform and taper ratio were selected, the primary design task was optimization of foil section properties to satisfy section thickness (structural) and cavitation (performance) criteria.

Initial plans called for a solid forward foil numerically machined from a block of steel. Further structural and hydrodynamic analysis, however, indicated the possibility of significant weight reduction for a thicker, built-up foil. A trade study evaluating the extra manufacturing costs against the amount of weight saved yielded a minimum section

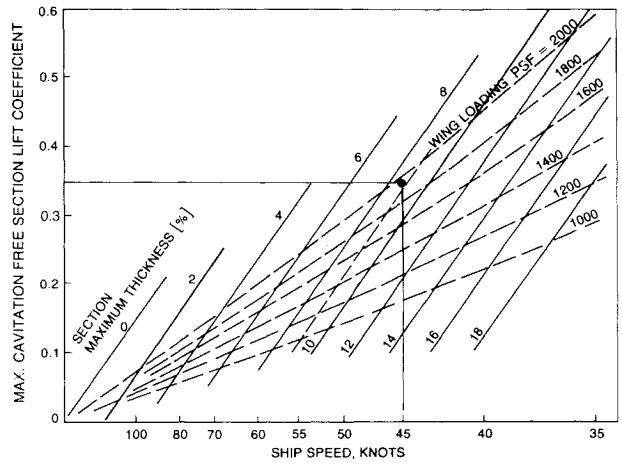

Fig. 5 Parametric foil design data for cavitation-free operation.

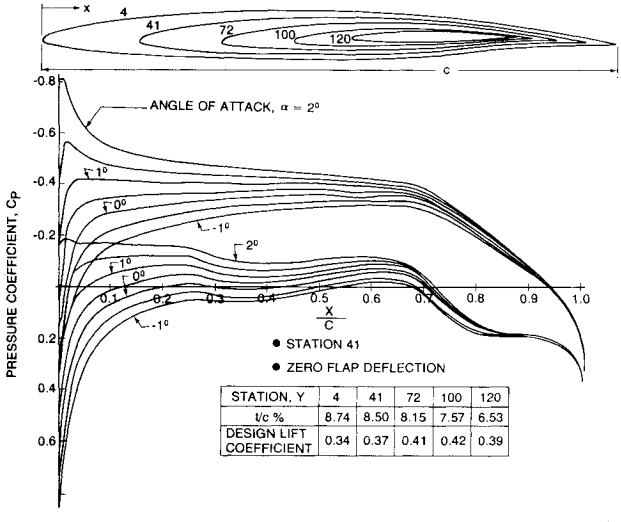

STATION, Y	4	41	72	100	120
t/c %	8.74	8.50	8.15	7.57	6.53
DESIGN LIFT COEFFICIENT	0.34	0.37	0.41	0.42	0.39

Fig. 6 Forward foil chordwise pressure distribution and section shape.

thickness ratio of 8.5% required at the structurally critical spanwise station, $Y=41$ in. Detailed analysis had indicated that for this particular foil configuration the stress level was highest at station 41.

The Model 929-115 forward foil spanwise variation of the section lift coefficient was obtained from three-dimensional potential flow analysis. As shown in Fig. 4, at spanwise station $Y=41$ the section lift coefficient and the foil lift coefficient happen to be practically identical. For this reason the section at foil station 41 was used to characterize the behavior of the complete foil configuration.

Parametric data on NACA series 16 foils[6] with a meanline of $a=0.8$, shown in Fig. 5, guided the initial design of the new foil sections. For a speed of 45 knots and an 8.5% section thickness, a lift coefficient of up to 0.35 could be generated before the onset of cavitation.

An 8.5% thick section was designed to provide low-pressure level, limited by cavitation considerations, over a large portion of the foil upper surface, as indicated in Fig. 6. The first 60% of the lower surface was shaped mainly for optimum structural characteristics. For additional lift, a region of high pressure was provided on the aft lower surface of the section. For an upper surface minimum pressure coefficient of -0.43, a maximum cavitation-free foil lift coefficient of 0.37 was achieved. Under normal operation the lift coefficient is well below that maximum. The section was designed for a lift coefficient higher than normally experienced in cruise to provide cavitation-free margin if the ship weight should be increased or in accelerated flight conditions such as climbing waves or tight turns.

The next task was to adapt this new two-dimensional section to the requirements of a three-dimensional foil. Outboard of station 41, the section local lift coefficients are as much as 16% higher than the overall foil lift coefficient, while inboard section lift coefficients are lower, as shown in Fig. 4. According to Fig. 5, the section thickness can be increased as the lift coefficient is lowered. Fortunately, this trend coincides with structural requirements. Near the foil root, where the wing bending moment is the highest, the thickest section is required. Conversely, thinner sections may be used farther outboard, where local lift coefficients are higher and bending moments are lower. Figure 6 shows the thickness ratios and the design lift coefficients selected for the sections defining the Model 929-115 forward foil. The camber of these sections varies with design lift coefficient. The three-dimensional potential flow program[3] was employed for the camberline design process. The forward foil was represented by a network of panels. A foil lift coefficient was prescribed and for each chordwise column of panels a weighting function for the chordwise load distribution was defined. The computer program calculated the panel orientation (slope) required to achieve this load distribution. Chordwise integration of the panel slopes yielded section camberline shape and angle of attack. An appropriate thickness distribution was applied to each of the section camberlines according to linearized airfoil theory. The resulting section shapes were then analyzed in two-dimensional potential flow.[5] Where necessary, the chordwise velocity distribution was modified and an improved section shape was determined using the mixed boundary conditions section design program.[4] The foil defining sections are shown in Fig. 6 in their installed attitude, which includes the geometric twist necessary to obtain a hydrodynamically untwisted foil. All forward foil angle-of-attack measurements are given relative to the foil reference plane. The chord lines of the defining sections are not necessarily parallel to this foil reference plane.

The two-dimensional potential flow analysis program[5] was employed to explore foil off-design characteristics (at station 41) for various angles of attack and flap deflection angles. At constant lift, downward flap deflections can cause a pressure peak at the upper surface hinge line, while upward flap deflections cause a foil leading-edge pressure peak, as shown in Fig. 7. Incipient cavitation is assumed to occur when the critical cavitation pressure level is reached anywhere on the section.

Figure 8 shows the minimum pressure coefficient as a function of the section lift coefficient, with flap deflection angle as a parameter. At small flap deflection angles and moderate lift levels, the minimum pressure occurred near the foil upper surface midchord. At higher section lift coefficients (higher angles of attack), a suction peak developed at the upper surface leading edge. This peak increased rapidly when the lift coefficient (angle of attack) was further increased. At low section lift coefficients (angles of attack), a similar peak formed at the lower surface leading edge. If the flap was deflected, a suction peak formed at the convex corner of the flap hinge line. In potential flow, the pressure at this sharp corner would be infinitely low. In real flow, however, the displacement thickness of the boundary layer smooths the flow around this corner. At larger flap deflection angles, the lowest pressure occurred at the flap hinge line.

Figure 8 also shows the relationship between section lift coefficient and minimum pressure coefficient for a local foil loading of 1410 psf, which is also the forward foil design loading. Intersections of the section minimum local pressure lines at constant flap deflection with the 1410 psf foil loading line in Fig. 8 are cross plotted in Fig. 9, labeled "incipient cavitation limit." The foil section is predicted to be free of cavitation when operated within the cross-hatched "incipient cavitation" boundary line.

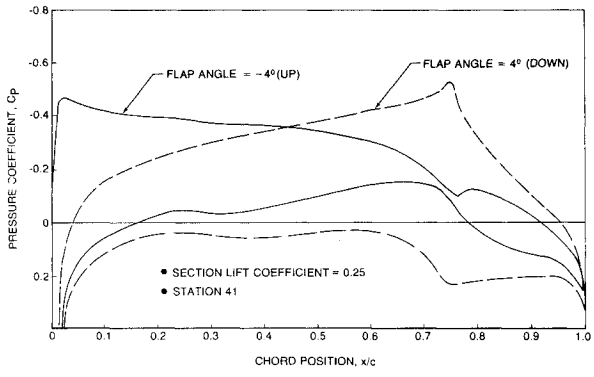

Fig. 7 Forward foil pressure peak relation to flap deflections.

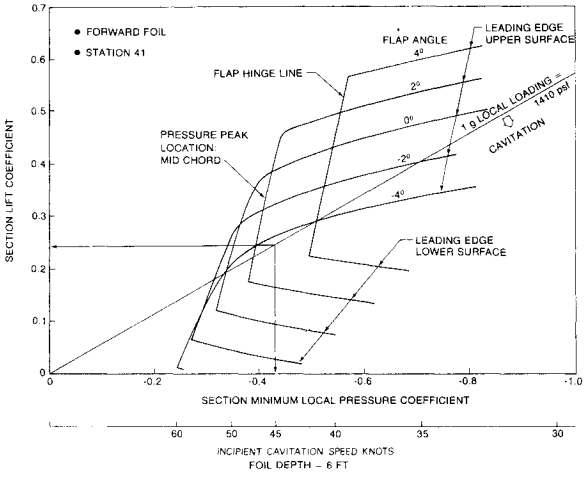

Fig. 8 Limiting cavitation conditions.

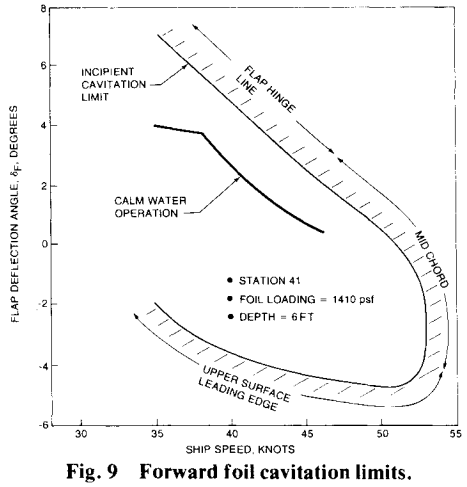

Fig. 9 Forward foil cavitation limits.

Aft Foil Design

The Jetfoil Model 929-115 aft foil planform remained unchanged, except for a small increase in chord length near the center strut for structural reasons. The basic section shape was slightly modified to provide more camber and a more uniform pressure distribution than the original Jetfoil section. Aft foil cavitation limits, derived in the fashion used for the forward foil, are shown in Fig. 10.

Off-Design Foil Section Characteristics

Jetfoil operates at constant dynamic lift over the foilborne speed range, therefore the foil experiences off-design lift coefficients at speeds other than 45 knots and ship weights

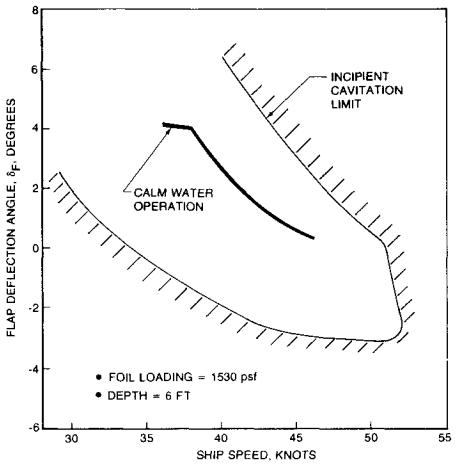

Fig. 10 Aft foil cavitation limits.

other than 112 long tons. Further, when operating in waves, the wave orbital velocities change both the angle of attack and dynamic pressure. The foil section must, therefore, be capable of satisfactory operation over a wide range of angle-of-attack and flap deflection excursions to provide constant lift for the ship.

The relationship between flap deflection angle and ship speed for trimmed flight at 112 long tons ship weight is shown in Figs. 9 and 10. Assuming that leading-edge cavitation is more detrimental than hinge line cavitation, the operating line matches the cavitation limit line reasonably well. Model 929-100 forward flap excursions measured in sea state 4 were 5.4 deg (two standard deviations). Similar deflections were expected for Model 929-115. At 40 knots ship speed, the theoretical flap deflection cavitation margin shown in Fig. 9 is 6.2 deg in the negative direction and 2.1 deg in the positive direction. Flap hinge line intermittent cavitation on the forward foil was, therefore, expected in sea state.

For Model 929-100, the aft flap excursions measured relative to their calm water equilibrium positions were 7.2 deg (two standard deviations) in sea state 4. At 40 knots ship speed, the theoretical flap deflections for cavitation incipience, measured relative to this neutral position, is 4.6 deg in the negative and 3.8 deg in the positive direction, as shown in Fig. 10. These deflections are less than the the expected flap excursions in a sea way, therefore some aft foil cavitation was anticipated in sea state.

Foilborne Drag Prediction

Prediction of Model 929-115 foilborne cruise performance was based upon Model 929-100 drag derived from propulsion system performance monitored during sea trials and calculated drag differences associated with foil system configuration changes from Model 929-100 to 929-115. Test stand thrust data were used to calibrate the Model 929-100 propulsion pumps.

Foil system induced drag differences were calculated using the three-dimensional potential flow computer program. Aerodynamic drag differences were derived from wind tunnel tests of 1/24 size Jetfoil models. Other drag changes were determined using classical empirical techniques.

Model 929-100 drag was also computed using theoretical and empirical relationships to indicate the relative importance of various sources of drag, as shown in Table 1. Sea trials of Model 929-100 showed agreement with the prediction within 1% up to 41.5 knots ship speed. Above 41.5 knots the drag inferred from thrust measurements exceeded the prediction, with a difference of 8% at 44 knots because of cavitation drag that was not modeled in the prediction. A credible cavitation drag model was not available.

The change in drag as a result of configuration differences was determined, as shown in Table 2. Elimination of the

Table 1 Calculated drag contributions, Model 929-100

Contributor	Percent of total drag
Forward foil	
Viscous	11.2
Induced	12.0
Aft foil	
Viscous	20.6
Induced	15.2
Struts	
Viscous	15.6
Spray	10.0
Wave	0.3
Pods	
Viscous	9.5
Wave	0
Aerodynamic	5.6
Ship speed = 40 knots	Ship weight = 110 long tons
Forward foil depth = 6 ft	

Table 2 Drag difference contributions

Model 929-115 compared to model 929-100 Ship speed = 43 knots Ship weight = 112 long tons		No wind
	Contributor	Drag difference, lb
Hull	Aerodynamic	−200
Forward foil	Induced	−970
	Viscous	580
	Spray	67
Aft Foil	Induced	500
	Viscous	−640
	Total	−663
Model 929-100 drag at 110 long tons	=	21,850
Correction for 112 long tons	=	250
Model 929-115 drag at 112 long tons		21,437

pilothouse sun screen for Model 929-115 was evaluated using scale-model wind-tunnel test data of Jetfoil configurations with and without a sun screen. Contributions of induced, viscous, and spray drag were determined to arrive at the difference in forward foil system drag between Models 929-100 and 929-115. Forward foil induced drag coefficients were calculated using three-dimensional potential flow analysis. The larger span of the Model 929-115 significantly reduced induced drag. Model 929-115 has a higher viscous drag because of the added foil area, strut chord length, and a 13 ft^2 increase in pod wetted surface area. Turbulent flat plate skin friction drag with corrections for skin roughness and body shape[7] were used to arrive at the viscous drag increment shown in Table 2. Forward strut spray drag was calculated by an empirical relationship relating drag coefficient to strut maximum thickness and chord length.

The difference in aft foil system drag between Models 929-100 and 929-115 was calculated as follows. Aft foil system induced drag consisted of drag caused by downwash generated by the forward foil and drag induced by the aft foil itself. Induced drag coefficients were calculated using the three-dimensional potential flow program. The aft foil system induced drag caused by downwash from the front foil depends on the location of the front foil wake relative to the aft foil and/or the amount of wake vorticity dissipated by the time the front foil vortices reach the aft foil system. These factors were not known, so the extremes of no interaction and maximum front-aft foil interaction were explored and finally a 20% dissipation of vorticity assumed. The larger span front foil of Model 929-115 affects a larger portion of the aft foil and, therefore, increased the aft foil induced drag compared to Model 929-100, as shown in Table 2.

The viscous drag of the Model 929-115 aft foil system was reduced by the use of smaller skegs, removal of all external stiffeners on the strut, and deletion of a flange fairing below the center strut. Scale-model wind-tunnel data for struts with and without flange fairing or stiffeners were used to assess the savings in drag. The drag difference because of skeg size reduction from 4.06 ft^2 for Model 929-100 to 2.36 ft^2 for Model 929-115 was calculated assuming flat plate turbulent skin friction. Total aft foil system profile drag reduction is given in Table 2. Since aft strut thickness did not change between models, the wave and spray drag were assumed to be unchanged. The deflection of the free water surface behind the front foil, calculated by the three-dimensional potential flow program,[2] was nearly identical for both forward foils, therefore no change in aft strut submergence and correspondingly no change in aft strut viscous drag was assumed.

The sum of drag changes between models is given in Table 2. Model 929-115 design cruise weight of 112 long tons is greater than Model 929-100 by 2 tons. Table 2 contains a drag adjustment, derived from Model 929-100 sea trials, to account for this weight difference. The predicted drag characteristics of Model 929-115 are shown in Fig. 11.

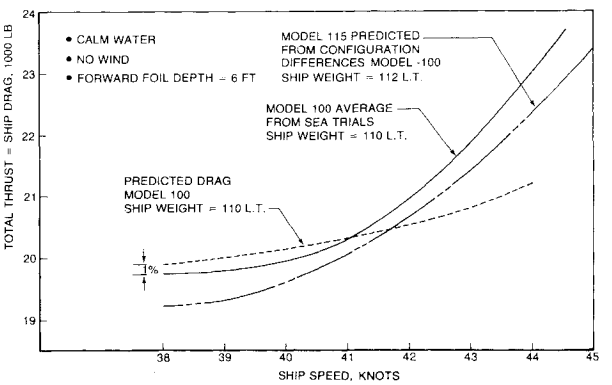

Fig. 11 Foilborne cruise drag.

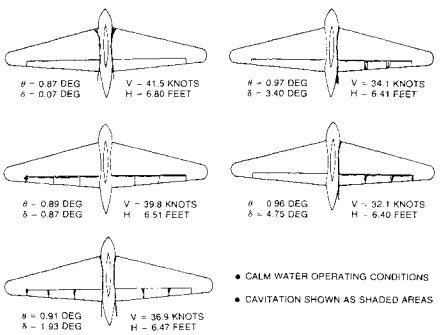

Fig. 12 Forward foil flowfield observations.

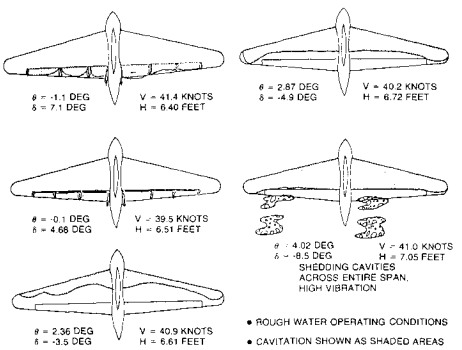

Fig. 13 Forward foil flowfield observations.

Sea Trial Flow Observations

Sea trials were conducted on Jetfoil 0011, the first Model 929-115, from June to October 1978. The flow over the front and aft foil systems was observed to detect cavitation or ventilation.

The forward foil system was observed during steady-state operation over an angle-of-attack range of 5 deg. Typical cavitation patterns for calm water operation are shown in Fig. 12. Except for a small amount of cavitation at the hinge line and at the foil-pod intersection, the new forward foil system was cavitation-free under calm water operating conditions.

Cavitation patterns shown in Fig. 13 are for conditions encountered during transients in rough water. Leading-edge cavitation extending over more than 40% of the foil chord was observed with no ship vibrations or measurable negative effects on performance. Leading-edge cavitation extending aft to the hinge line became unstable, broke free, and shedded downstream. This flow instability caused high-amplitude ship vibrations. At lower angles of attack, associated with positive flap deflections, cavitation appeared on the flaps, beginning near the flap hinge line. The appearance of this cavitation was not accompanied by vibration but probably contributed to reduced flap effectiveness.

Cavitation patterns, ship attitude, speed, and flap deflection were related as shown in Fig. 14. The cavitation margin was adequate to ensure cavitation-free operation during normal calm water cruise operation.

Flap deflections observed during operations of Jetfoil 0011 in upper sea state 4 are also shown in Fig. 14. These excursions, representing two standard deviations of the observed flap travel, are greater than the calculated or observed cavitation-free flap deflection limits, resulting in leading-edge and hinge line cavitation on the forward foil in sea state 4 about 20% of the time.

The aft foil system was observed during steady-state operation over an angle-of-attack range of 7 deg. Typical cavitation patterns for the visible portions of the aft foil are described in Fig. 15 for calm water operation.

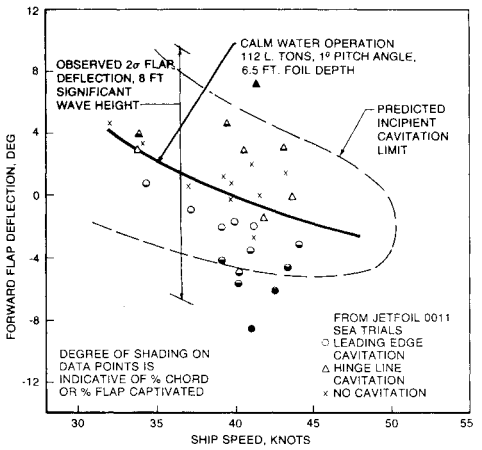

Fig. 14 Forward foil cavitation experience.

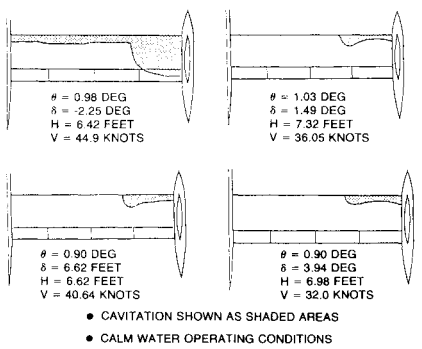

Fig. 15 Aft foil flowfield observations.

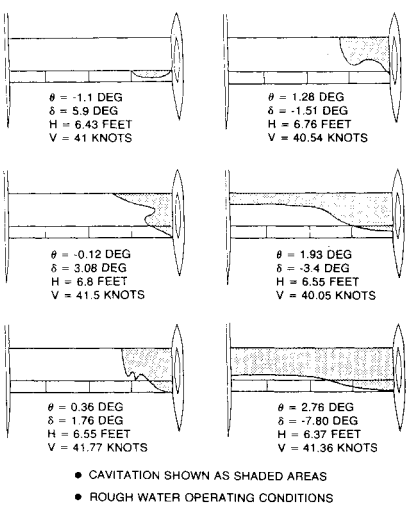

Fig. 16 Aft foil flowfield observations.

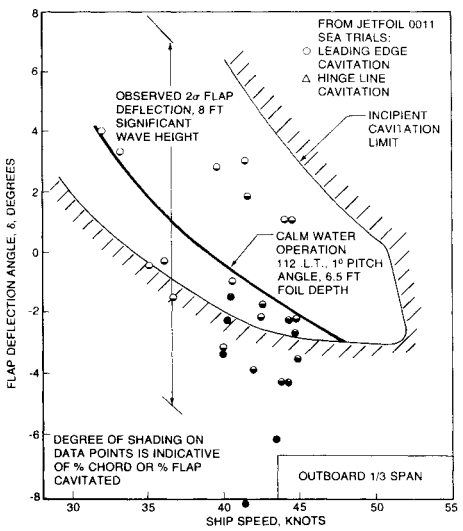

Fig. 17 Aft foil cavitation experience.

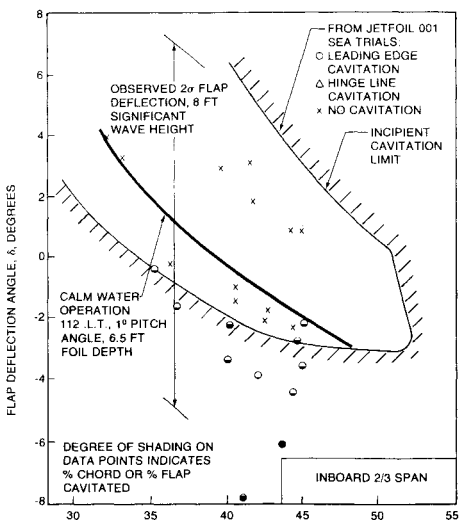

Fig. 18 Aft foil cavitation experience.

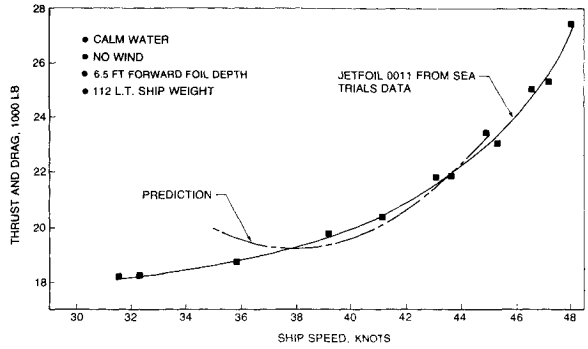

Fig. 19 Thrust and drag relationship to ship speed.

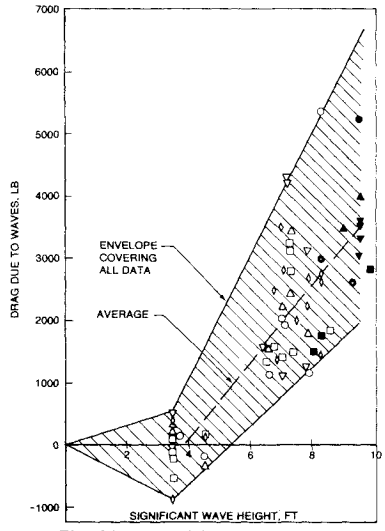

Fig. 20 Sensitivity to waves.

The forward foil creates a highly nonuniform inflow field to the aft foil, which is manifested in Fig. 15 by distinctly different cavitation patterns between the inboard two-thirds of the panel and the outboard one-third. The angle of attack of the flow approaching the outboard portion of the aft foil is higher than at the inboard portion, because of the downwash and upwash from the forward foil. During normal operation at speeds up to about 42 knots, the aft foil was cavitation-free on the inboard two-thirds of the foil but carried leading-edge cavitation on the outboard one-third of the panel. Cavitation patterns are shown in Fig. 16 for conditions that might be encountered during transients in rough water. Cavitation was present mainly on the outboard one-third of the panel, except for inboard leading-edge cavitation at ship pitch angles above 1.5 deg.

Cavitation patterns for the aft foil were related to ship attitude, speed, and flap deflection. The results were plotted in Fig. 17 for the inboard two-thirds of the foil panel and in Fig. 18 for the outboard one-third of the foil panel. For the inboard two-thirds span, agreement of observations with predictions is excellent. For the outboard one-third span, observed leading-edge cavitation is more extensive than predicted. Hinge line cavitation observed was consistent with the prediction. Aft flap deflections in upper sea state 4 for Jetfoil 0011 were nearly coincident with the hinge line cavitation limit but extended beyond the leading-edge cavitation limit. Leading-edge cavitation was therefore experienced on the aft foil while operating in sea state 4 about 25% of the time.

Foilborne Ship Performance from Sea Trials

Foilborne cruise performance evaluation of Jetfoil 0011 in the 1978 sea trials involved calculation of basic ship drag, determination of the sensitivity to ship weight, foil depth, waves, winds, and foil incidence angles, as well as speed-power and fuel consumption relationships. Only those parameters directly related to foil hydrodynamic performance are presented.

Drag (from thrust) of Jetfoil 0011 in sea trials compared to prediction is shown in Fig. 19.

Through most of the speed range, thrust calculated from sea trial measurements was within 2% of the predicted drag, with the thrust, and therefore the "measured" drag, being lower than predicted at low ship speeds. Sensitivity to ship weight over the speed range was about 125 lb of drag per long ton. Sensitivity to foil depth, for depths greater than 5 ft, was 500 lb of drag per foot submergence. Sensitivity to forward foil incidence angle was small in the region near the 2 deg setting. Sensitivity to aft foil incidence angle was small for angles of 1.3-2 deg, with drag increasing for angles above 2 deg, therefore 2 deg was selected for both forward and aft foil incidence angles.

Foilborne cruise performance in rough water was independent of ship heading but, as shown in Fig. 20, was dependent upon wave height. Scatter in the data was large. Wave period was not separable as a test variable and could be a major contributor to data variability. The increased drag above a significant wave height of 4 ft may be partly a result of added hull drag from increased frequency of hull "cresting" as wave height increases. Continuous foilborne operation was possible at most headings in waves up to 9.5 ft of significant wave height.

Conclusions

The following conclusions were derived from Jetfoil 0011 sea trials and supportive analyses:

1) Predicted drag was within 2% of the drag deduced from foilborne cruise sea trials.

2) Jetfoil 0011's forward foil was cavitation-free in normal foilborne operation. Agreement of observed cavitation with predictions was adequate. Leading-edge cavitation less than 50% chord had no detectable influence on ship vibration or ride quality.

3) Predictions agreed with the observed cavitation on the aft foil for the inboard two-thirds span and for the hinge line of the outboard one-third span.

4) Ship drag, as predicted, was sensitive to ship weight and foil depth. Drag was influenced by aft foil incidence angle but was insensitive to a ship pitch angle change of 0.5 deg. Added drag in waves was independent of ship heading relative to sea direction but was dependent on wave height.

5) Contouring the forward pod and careful strut and foil section theoretical design provided sufficient margin with respect to cavitation.

References

[1] Shultz, W.M., "Boeing Jetfoil Report," Paper presented at AIAA/SNAME 2nd Advanced Marine Vehicles Conference, Feb. 1974.

[2] Rubbert, P. E., Saaris, G.R., Scholye, M.B., Standen, N.M., and Wallace, R.E., "A General Method for Determining the Aerodynamic Characteristics of Fan-in-Wing Configurations," USAAV Laboratories, Technical Report 67-61A, 1967.

[3] Feifel, W.M., "Three-Dimensional Potential Flow Analysis-Design-Optimization Program A372," Boeing Document D321-51510-1, 1979.

[4] Johnson, F.T. and Rubbert, P.E., "Advanced Panel-Type Influence Coefficient Methods Applied to Subsonic Flows," AIAA Paper presented at AIAA Aerospace Sciences Meeting, Pasadena, Calif., 1975.

[5] Feifel, W.M., "Two-Dimensional Flow Analysis and Jet Flap Simulation Program TEA304B," Boeing Document D643832TN, 1976.

[6] Abbott, I.H. and Von Doenhoff, A.E., *Theory Wing Sections—Including a Summary of Airfoil Data,* Dover Publications, Inc., New York, 1959.

[7] Hoerner, S.F., *Fluid Dynamic Drag,* published by the author, 1965.